Effect of clad height, substrate thickness and scanning pattern on cantilever distortion in direct metal deposition

Fabian Soffel[1] · Daniel Eisenbarth[1] · Konrad Wegener[2]

Abstract

In metal additive manufacturing, moving heat sources cause spatial and time-dependent variations of temperature and strain that can lead to part distortions. Distortion prediction and optimized deposition parameters can increase the dimensional accuracy of the generated components. In this study, an analytical approach for modeling the effect of clad height and substrate thickness is experimentally validated. Additionally, the influence of the scanning pattern as a function of clad height and substrate thickness is determined experimentally. The analytical model is based on the cool-down phase mechanism and assumes the formation of constant thermal shrinking forces for each deposited layer. The model accurately predicts longitudinal cantilever distortion after experimental calibration when compared with similar experimental conditions. For multi-layer deposition, the scanning pattern has the largest influence on distortion for thin-walled substrates. An optimized deposition strategy with longitudinal scanning vectors leads to a distortion reduction of up to 86%. The results highlight the potential of mechanical modeling and scanning strategy optimizations to increase the shape accuracy for industrial applications in the field of additive manufacturing.

1 Introduction

Direct metal deposition (DMD) is an additive manufacturing (AM) technology based on laser powder deposition welding. The energy and aerospace industries apply DMD for coatings and repair welds of high value components since many years. Recent technological advancements in machine tool and software development allow the fabrication of entire complex-shaped parts, such as closed pump impellers [1]. However, metal additive manufacturing poses various scientific, technological, and economic challenges [2]. For DMD process development, some of the main challenges are layer height instabilities, defect formations, anisotropic mechanical properties, residual stress, and distortions [3]. The powder nozzle design influences the self-stabilization characteristics of the DMD process, which is essential to prevent layer height instabilities [4]. Defect prevention is mainly linked to the choice of powder material and process parameters. To minimize anisotropy of mechanical properties, the direction of the individual welding tracks is typically varied during the part buildup. Woo et al. [5] showed that an alternation of the scanning direction for each new layer or an island scanning strategy result in a less preferentially inclined grain structure and a smaller range of residual stress values compared to a constant bidirectional pattern. Residual stress and distortion arise from transient temperature fields that are generated by the moving heat source [6].

The DMD manufacturing strategies can be optimized to handle the aforementioned challenges. Ng et al. [7] analyzed porosity formation and showed that the melt pool flow strongly affects the overall part density. Wirth [8] demonstrated that an increased interaction time of the laser radiation with the melt pool increases the density, as the longer lasting fluid motion of the melt supports the escape of entrapped gas. To increase the built rate, surface quality, and shape accuracy of

✉ Fabian Soffel
  soffel@inspire.ethz.ch

  Daniel Eisenbarth
  daniel.eisenbarth@gmail.com

  Konrad Wegener
  wegener@iwf.mavt.ethz.ch

[1] inspire AG, ETH Zürich, Technoparkstrasse 1,
  8005 Zürich, Switzerland

[2] Institute of Machine Tools and Manufacturing, ETH Zürich,
  Leonhardstrasse 21, 8092 Zürich, Switzerland

parts manufactured by DMD, the process can be combined with conventional manufacturing techniques. Soffel et al. [9] showed that casting, milling, and DMD can be combined to fabricate parts efficiently and with mechanical properties exceeding conventional manufacturing methods. As highlighted by Eisenbarth et al. [10], the process sequence for the combination of additive and subtractive manufacturing is of high importance for the dimensional accuracy of the final part. The DMD process induces residual stress that before or after machining can lead to part distortions that are orders of magnitude larger than the milling accuracy. Therefore, it is of high interest to further investigate distortion formation in DMD manufacturing processes.

The origin of distortions is important to examine to develop process strategies for their minimization. Gray et al. [6] described how thermal dilatation of welded material leads to differential strain fields that result in part distortions. Mukherjee et al. [11] showed how the susceptibility to thermal strain can be evaluated for different materials and found that Ti6Al4V is more susceptible to distortion than IN625. Heigel et al. [12] identified two main modes of substrate distortion during laser cladding: longitudinal bending and transverse angular distortion. Longitudinal bending occurs along and angular distortion perpendicular to the scanning direction of an individual welding track. For the experimental analysis of substrate distortion during DMD, typically one edge of the base plate is fixed while the remaining part is free to deform [12–17]. This cantilever setup is the preferred experimental method as the well-defined mechanical boundary conditions allow direct comparison with mechanical models.

For the prediction of residual stress and distortion, a variety of models have been developed that can be distinguished between numerical and analytical approaches. Yang et al. [18] presented a FEA-based thermo-mechanical model that could predict cantilever distortion after deposition of a rectangular DMD structure of five layers. Xie et al. [19] developed a numerical model with layer-by-layer element activation and found that computational time could be reduced by a factor of greater than 10 compared to conventional step-to-step element activation. Biegler et al. [20] analyzed shape deviations during the fabrication of a turbine blade consisting of 80 layers using the commercial software Simufact Welding. They showed that the application of the simulation results for distortion compensation could increase the geometrical accuracy of the final part. One main challenge in numerical modeling is the large amount of computational time that is required for the prediction of the thermo-mechanical behavior. As alternatives, analytical modeling approaches were developed that require only a fraction of computational costs. Yan et al. [16] predicted the angular distortion of a cantilever analytically using an equation derived by Shen et al. [21] originally developed for laser forming based on the temperature gradient

mechanism. However, this equation can only predict the angular distortion mode and can therefore not be applied to deposition strategies with alternated scanning directions. Another approach based on the cool-down phase model was defined by Mercelis and Kruth [22] for the prediction of residual stress during powder bed fusion. This cool-down phase mechanism relates the thermal shrinkage of each deposited layer to the formation of residual stress and distortions in the overall structure. To the knowledge of the authors, the application of the cool-down phase model could not yet predict longitudinal bending of cantilevers for varying experimental conditions in DMD. Such an approach could be helpful to develop distortion mitigation strategies at very low computational costs.

Numerous studies experimentally quantified the substrate distortion as a function of DMD process conditions. The varied parameters included energy input, scanning speed, inter-layer dwell times, DMD structure, substrate geometries, and scanning patterns (Table 1). Yan et al. [16] and Mukherjee et al. [23] found that increased energy inputs either by increased laser power or reduced scanning speed lead to larger distortions. The effect of inter-layer dwell times was studied by Denlinger and Michaleris [17], and it was shown that increased cooling times result in smaller distortions for IN625, but larger distortions for Ti6Al4V, which could be related to differences in material properties. Concerning the effect of the DMD structure geometry, Xie et al. [24] studied how substrate deflections increase for longer welding tracks and Liang et al. [25] observed increased distortion for larger structures with a higher number of deposited layers. Yan et al. [16] varied the thickness of a cantilever from 5 to 10 mm for transversal scanning and showed that distortion is decreased significantly with increased substrate thickness. Regarding the scanning strategy, they found that the maximum deflection after transversal scanning was 7.6 times larger compared to longitudinal scanning. Ren et al. [13] measured 2.3 times greater plate deflection with a transversal scanning pattern for a constant substrate thickness of 3 mm. In both last-mentioned studies, the substrate thickness was not varied to evaluate the influence of the deposition pattern, so the interaction of these two parameters could not be detected. Heigel et al. [12] tested the influence of the deposition pattern on cantilever tip distortion for 3 different process parameter combinations for 6.35-mm-thick substrates. For two parameter sets, the longitudinal scanning strategy caused an increase of total deflection of 10% and 49%, respectively, whereas for another set of parameters it decreased for 11% compared with transversal scanning. Since these experiments were performed with constant substrate thickness and clad height, the effect of the scanning pattern could not be evaluated as a function of substrate and deposit geometries. It is expected that such an analysis can lead to optimized DMD manufacturing strategies that result in distortion reduction.

Table 1 Effect of DMD process conditions on cantilever distortion according to literature [12, 13, 16, 17, 23–25]

Input parameter	Variation method	Effect on distortion	Ref.
Energy input	Laser power increase	Increased	[16, 23]
Scanning speed	Scan speed increase	Increased	[16, 23]
Inter-layer dwell-time	Dwell-time increase	Decreased (IN625)	[17]
		Increased (Ti6Al4V)	[17]
DMD geometry	Size increase	Increased	[24, 25]
Substrate geometry	Thickness increase	Increased	[16]
Scanning strategy	Longitudinal	Increased	[12]
		Decreased	[12, 13, 16]

In the present study, it is investigated how analytical modeling can predict and how deposition strategy optimizations can reduce cantilever distortions. There are two main aims of the study: First, a simplified analytical model based on the cool-down phase mechanism is developed to predict longitudinal bending as a function of clad height and substrate thickness. Second, the effect of the scanning strategy is analyzed experimentally as a function of substrate thickness and deposit height as a basis for deposition strategy optimizations. In summary, the analytical model can effectively predict substrate bending and the experimental results show that for very thin substrates transverse scanning leads to significant larger distortions compared to longitudinal scanning, whereas for thicker substrates the scanning pattern influence is reduced. The paper is structured as follows: Section 2 describes the analytical modeling approach and the experimental procedures. Section 3 presents and discusses the modeling results and validation first and then the effect of scanning strategies. Finally, Section 4 summarizes the conclusions of the most relevant findings.

2 Materials and methods

2.1 Analytical modeling approach

A simplified theoretical model considering the cool-down phase mechanism was used to predict longitudinal distortion after layer deposition with a longitudinal scanning strategy. Figure 1 illustrates the model definitions. The model is based on the general beam theory where a bending moment

$$M_y = L_c(n)F_x = EI_y(n)\frac{d2u_{z,n}(x,n)}{dx2} \tag{1}$$

results from longitudinal shrinkage forces F_x at a distance L_c to the area center after the deposition of each layer. This moment causes the material to bend along the central path $u_{z,n}(x,n)$ depending on its Young's modulus E and the geometrical moment of inertia I_y, which is increasing with the number of layers n.

When applying the boundary conditions $u_{z,n}(x{=}0) = u'_{z,n}(x{=}0) = 0$ the bending line

$$u_{z,n}(x,n) = \frac{L_c(n)F_x x^2}{2EI_y(n)} \tag{2}$$

can be obtained with

$$L_c(n) = t + w - \frac{wt^2 + ab^2(n)}{2wtab(n)} \tag{3}$$

and

$$I_y(n) = \frac{wt^3}{12} + z_1^2(n)wt + \frac{ab^3(n)}{12} + z_2^2(n)ab(n) \tag{4}$$

with the geometrical values a, b, w, t, z_1, and z_2 according to Fig. 1. Since the touch probe measurements were performed at a distance $L_{lin} = 3$ mm from the DMD structure, the maximum cantilever tip deflection

$$u_{z,n,max}(n) = u_z(L,n) + u_{lin}(n) = \frac{L_c F_x L^2}{2EI_y(n)} + \frac{du_z(L,n)}{dx}L_{lin} \tag{5}$$

can be calculated with the deflection where x equals the length L of the layer and an additional linear term u_{lin}. The bending line for a multi-layer deposit

$$u_z(x) = \sum_{n=1}^{n_{tot}} u_{z,n}(x,n) \tag{6}$$

is then calculated by the sum of each individual layers contribution. The value for F_x/E is determined experimentally for model calibration. Thereby, it is assumed that the shrinking forces caused by each deposited layer are constant.
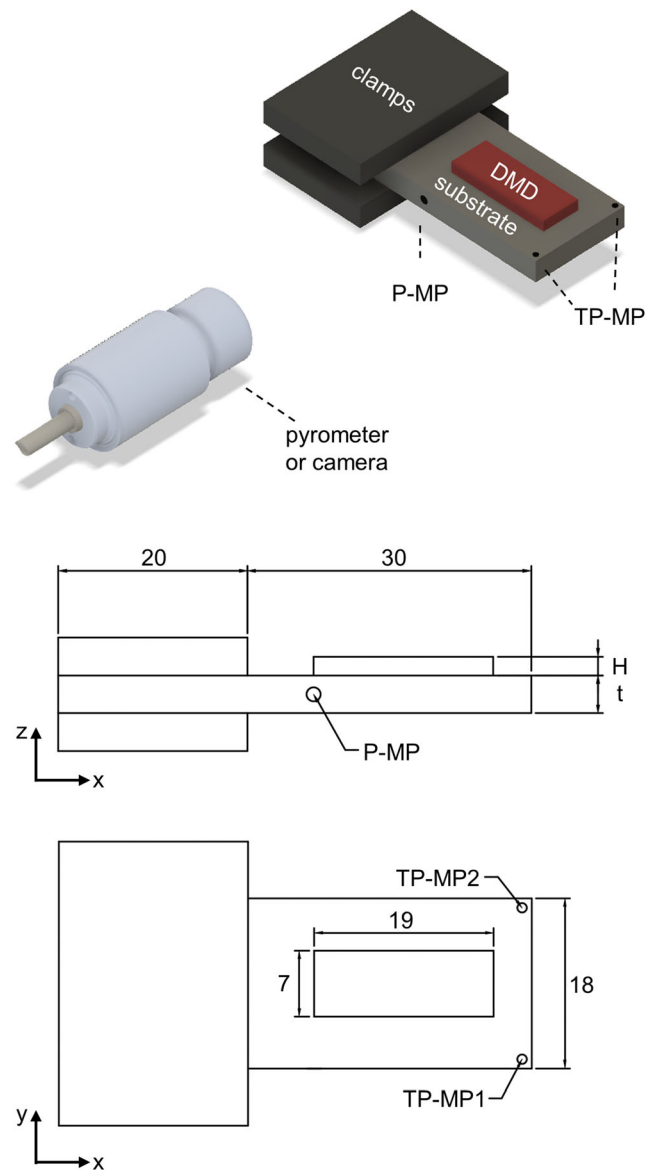
2.2 Experimental setup

A 5-axis machining center Mikron HPM 450U by GF Machining Solutions equipped with laser processing components was used for the laser cladding experiments. The components include an IPG Photonics 1 kW YLR-1000 fiber laser system with a wave length of 1070 nm and a Hybrid Manufacturing Technologies (HMT) processing head with a
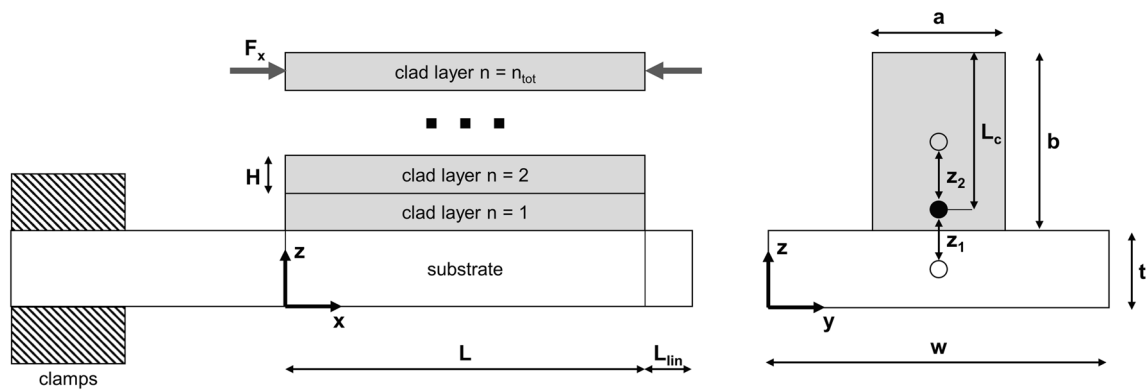
Fig. 1 Definitions of the analytical modeling approach for the analysis of longitudinal cantilever bending

laser spot size of about 1 mm that can be mounted into the spindle of the machine tool. Mild steel S235JRC (1.0122) substrates were clamped on one side as a cantilever as illustrated in Fig. 2 and oriented with a touch probe such that bending deformation is likeliest to occur around the Y axis of the machine tool. The substrate thickness was varied in five steps from 2 to 6 mm. Gas atomized nickel-based alloy Inconel 718 powder with a particle size between 45 and 105 μm and a chemical composition according to Table 2 was used as cladding material. The scanning speed and the powder flow rate were kept constant at 450 mm/min and 2.3 g/min, respectively. Each cladding layer had a width of $a = 7$ mm and a length of $L = 19$ mm. The laser scanning vectors were either aligned parallel (0°) or perpendicular (90°) to the longitudinal cantilever direction. With a 0.5-mm overlap of the single welding tracks, there were either 13 longitudinal or 37 transversal tracks in total to form one layer. The processing head was raised each layer by a z-increment of 0.62 mm. The clad height was varied by deposition of 1 to 6 DMD layers. The substrate distortion was measured both during laser cladding with a video camera as well as before and after the deposition process with a touch probe inside the machine tool. The touch probe measurements were performed at the two edge points of the substrate as illustrated in Fig. 2, and the average distortion values of those points in Z direction were calculated. The maximum distortion of one substrate edge point obtained in number of pixels by video camera was converted into mm to compare it with the touch probe measurement results. An infrared pyrometer Optris PI 3MH2 with a wavelength of 2.3 μm, a spot size of 1.5 mm, and a temperature range from 200 to 1500°C was used to measure the temperature on the substrate side during deposition at a distance of 150 mm.

In the first part of this study, the deposition strategy was kept unchanged. Each layer was deposited with 13 welding tracks parallel to the X axis. The X and Y coordinates of the end points of the odd layers were used as start points of the even layers and vice versa. Figure 3 illustrates this 0°/0° scanning strategy. In the second part of the study, the 0°/90°, 90°/0°,

Fig. 2 Setup for the experimental analysis of cantilever distortion with indication of the measurement points of the touch probe (TP-MP) and pyrometer (P-MP)

Table 2 Chemical composition of the Inconel 718 powder

Element	Fe	Ni	Cr	Nb+Ta	Mo	Ti	Al	C	N	O
wt.%	bal.	53.02	18.99	5.11	3.0	0.95	0.49	0.04	0.02	0.01

and 90°/90° scanning strategies were analyzed with in-situ measurement results of the video camera and pyrometer for substrate thicknesses of 2 mm, 3 mm, and 4 mm. Selected samples were further examined by metallographic investigations. Three-dimensional distortions were determined with a GOM ATOS Core 135 system.

3 Results and discussion

3.1 Analysis of longitudinal bending

The analytical model was initially calibrated with experimental data. For the calibration, the condition of 2-mm substrate thickness and one deposited layer was selected that leads to an average cantilever distortion of 0.45 mm. The calibration value of $F_x/E = 0.03448$ mm^2 was determined for this condition and remained constant in order to predict the deflection for increased substrate thickness and clad height.

Figure 4 shows the simulative and experimental results. There is a large effect of both substrate thickness and clad height on final cantilever deflection. Distortion significantly increases with a decrease of substrate thickness and an

increase of clad height similar to the findings of Yan et al. [16]. For thicker substrates, the distortion does not increase anymore considerably after deposition of the third layer. While the analytical model does predict the final distortion for $t = 2$ mm and 3 mm quite well with deviations between 2 and 13 %, the model deviations become large for increasing substrate thicknesses. From this result, it can be concluded that for thin substrates both shrinkage forces and the materials resistance against deformation remain on a similar level for up to three deposited layers in the investigated setup. Therefore, it is possible to predict longitudinal substrate bending very efficiently with the proposed analytical approach for conditions that are similar to the conditions under which the model was initially calibrated. However, for major changes of the experimental conditions, the model does not allow accurate predictions. For an increasing substrate thickness, the shrinkage forces caused by the thermal gradients might remain on a comparable level for the first layers, but the resistance of the material will increase due to less through-heating of the substrate and thereby a higher yield strength, which is not considered in the simplified model. For multiple layers at some point, the temperature of both the substrate as well as the already deposited structure will be significantly increased,

Fig. 3 Schematical overview of the four analyzed scanning strategies with indication of the deposition start (S) and end (E) for each layer
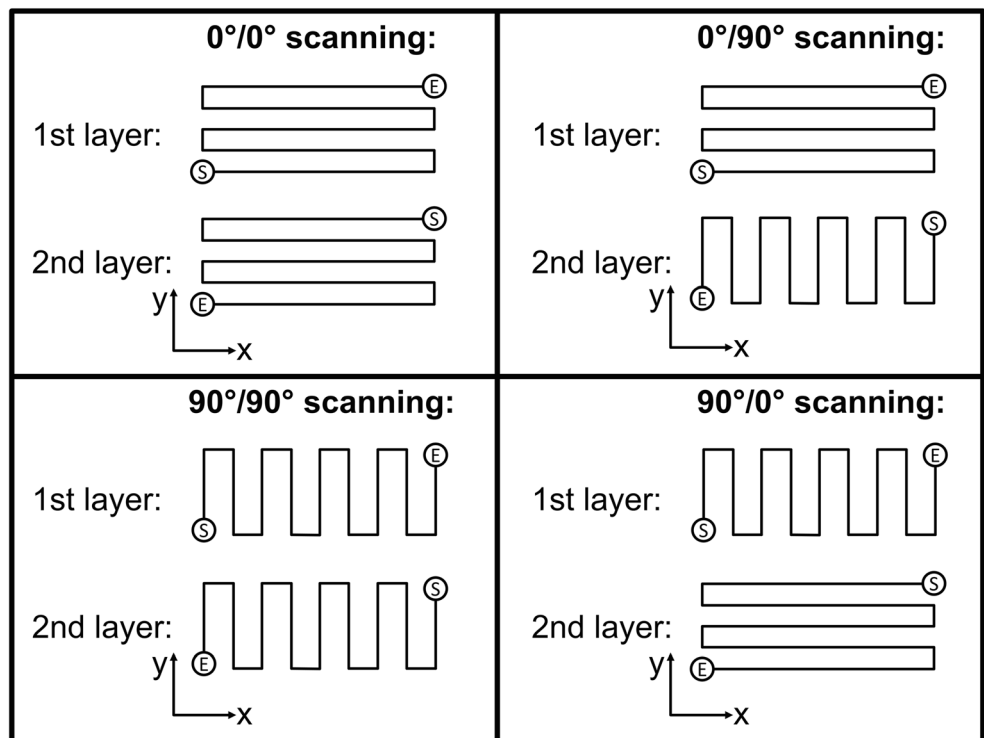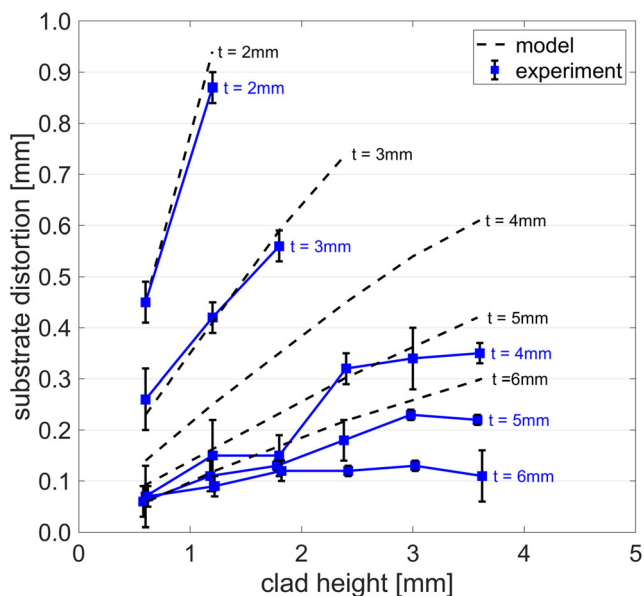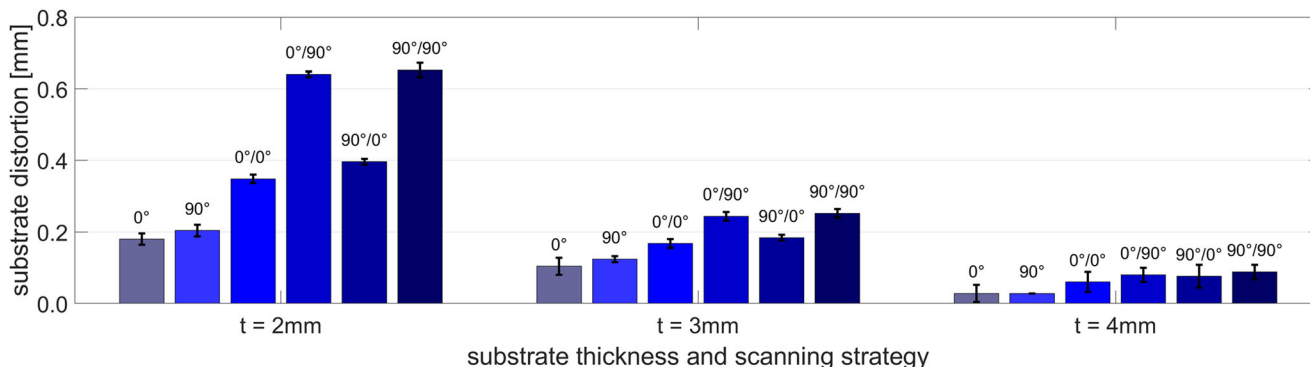
Fig. 4 Modeling and experimental results of final substrate distortion as a function of clad height and substrate thickness. Mean values and standard deviations are measurements of three specimens for each condition (*n*=3)

such that the shrinkage forces of additional deposited layers might not cause significant additional substrate distortion. These findings can be of high interest for industrial applications that require laser cladding on thin surfaces: As the first deposited layers are dominant for part deflection, they could be deposited with processing parameters that lead to a minimum amount of distortion, while the following layers could be deposited with parameters optimized for a high deposition rate. Such an approach could increase both shape accuracy and deposition performance for industrial laser cladding applications.

3.2 Effect of scanning strategies

The influence of the deposition pattern on the final substrate tip distortions is illustrated in Fig. 5. The scanning strategies

0° and 90° refer to the deposition of one single layer, whereas 0°/0°, 0°/90°, 90°/0°, and 90°/90° refer to two deposited layers according to Fig. 3. The experimental data originates from 54 individual deposited samples and the average values for three specimens per point are shown with their standard deviation. Similarly to the results of Ren et al. [13], transversal scanning leads to a larger amount of distortion than longitudinal scanning. For a single layer structure, the scanning vector orientation does have only a slight influence. However, the deposition pattern of the second layer strongly affects the final amount of distortion of thin-walled substrates in this study. Compared to the longitudinal 0°/0° scanning, the 0°/90° and 90°/90° strategies result in an increase of 83 % and 86% for *t* = 2 mm, 47% and 50% for *t* = 3 mm, and 35% and 50% for *t* = 4 mm, respectively. Compared to the 0°/90° deposition pattern, the 90°/0° strategy results in a distortion reduction of 62% for *t* = 2 mm, 33% for *t* = 3 mm, and 5% for *t* = 4 mm, respectively. As this finding can be of high interest for the selection of DMD deposition strategies, it is further analyzed with in-situ distortion measurements.

Figure 6 compares the in situ distortion measurement results of four different scanning strategies. The distortion increase of the 0°/90° and 90°/90° strategies occurs mainly in the second half of the second layer. From the tool paths in Fig. 3, it can be seen that the final tracks of the last-mentioned patterns have the largest distance to the free substrate edge. Therefore, angular distortion modes result in a larger edge deflection. Additionally, the local substrate temperature around the melt pool is increasing during deposition. The minimum temperature measurable by the pyrometer was 200°C, such that with this experimental setup only fragments of the substrate temperature could be observed during deposition. The highest temperatures were obtained with the 0°/0° pattern, where the interaction time with the material adjacent to the measurement point (P-MP in Fig. 2) was largest. These results indicate that during the deposition, the local substrate temperature is significantly increased over time, which leads to a reduced resistance of the substrate against deformation. This is believed to be the reason

Fig. 5 Experimental results of final substrate distortion as a function of substrate thickness and scanning strategy. 0° and 90° refer to the deposition of one single layer, 0°/0°, 0°/90°, 90°/0°, and 90°/90° to two deposited layers. Mean values and standard deviations are measurements of three specimens for each condition (*n*=3)
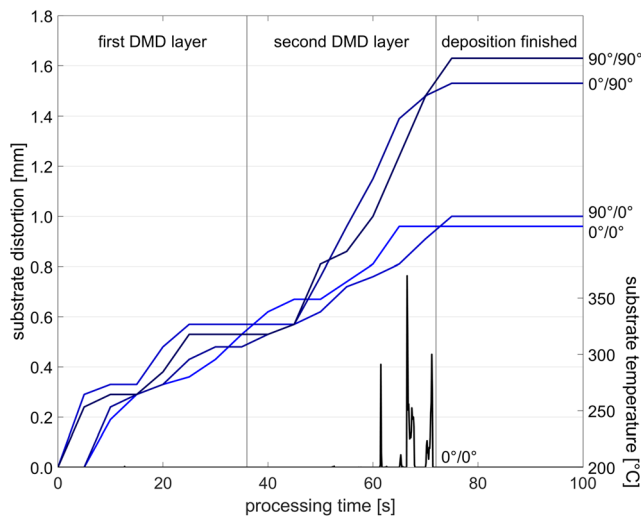
Fig. 6 In situ distortion and temperature measurement results of 2-mm-thick substrates for different scanning strategies

why the substrate tip deflection caused by angular distortion of the welding tracks perpendicular to the X axis is much larger for the second layer and may explain why the final distortion for the 0°/90° and 90°/90° strategies is greater than for the 90°/0° pattern. The results clearly show that the selected deposition strategy has a large influence on part deflection for laser cladding on thin-walled base material and highlight the potential of scanning pattern optimization.

Two metallographic specimens were analyzed in polished condition for evaluation of volumetric defects and validation of the modeling results for longitudinal bending. Figure 7 compares the cross sections of 2-mm-thick substrates after deposition of two layers with the 0°/0° and 90°/90° scanning pattern and the modeled bending line for the longitudinal

distortion mode. For both samples, the level of porosity is very low and the dilution to the substrate is uniform. The bending lines are significantly different: For the 0°/0° sample, the line is rather smooth, similar to what was predicted by the model and also shown in other research studies for example by Xie et al. [24]. The bending line of the 90°/90° sample has a more varying slope. This finding supports the assumption that the overall tip deflection for transversal scanning is caused by angular distortions as described by Heigel et al. [12]. The contribution of each individual welding track greatly varies over time due to the change in temperature and the distance from the tracks to the cantilever tip. The results of the metallographic investigation confirm the applicability of the selected process parameters for industrial purposes due to the high bonding quality and absence of critical volumetric defects.

The comparison of the modeled bending line and the cross section of the 0°/0° sample in Fig. 7 shows that the model is over-estimating the distortion. This can be explained with the fact that the model was calibrated with touch probe measurement results at the edge points of the substrate, whereas the cross section shows the middle of the sample. For the 0°/0° strategy however, additionally to the longitudinal distortion mode causing the substrate to bend around the Y axis, there is an angular distortion mode which results in a deflection angle around the X axis. Therefore, the total deflection is higher at the edges than in the middle for this deposition pattern. The 3D measurement results as illustrated in Fig. 8 confirm this assumption.

The results reveal limitations of this study regarding both the modeling and the experimental approach. The simplified analytical model can only predict distortions under conditions that are similar to the calibration
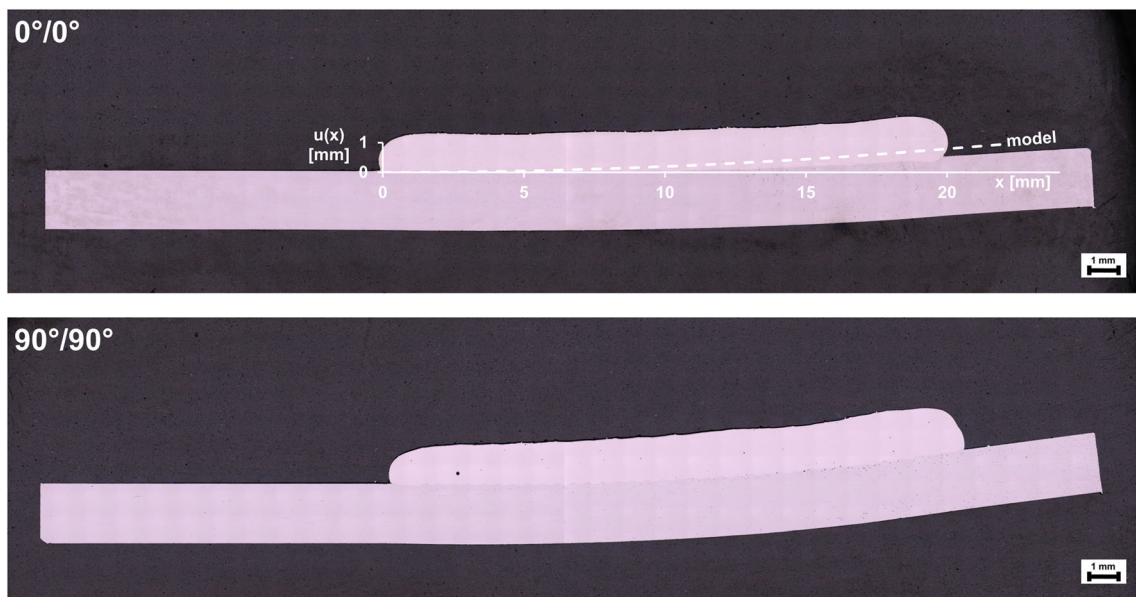
Fig. 7 Metallographic analysis of 2-mm-thick substrates for longitudinal (0°/0°) and transversal (90°/90°) scanning strategies
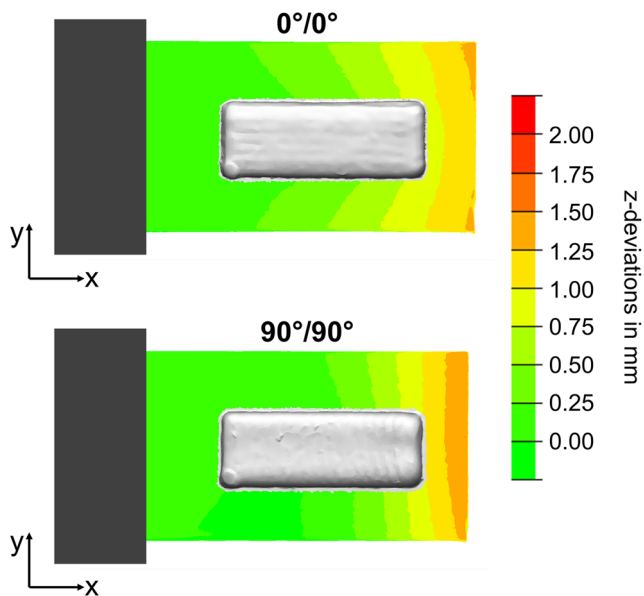
Fig. 8 3D scanning results of 2 mm thick substrates for longitudinal (0°/0°) and transversal (90°/90°) deposition strategies

conditions. For the distortion prediction of more complex geometries, FEA-based thermo-mechanical models as applied for example by Biegler et al. [20] should be considered. For further experimental analysis of in situ cantilever distortion, displacement could be measured by displacement sensors rather than a video camera and temperature by sensors that cover the full expected temperature range. These adjustments can facilitate the validation of thermo-mechanical models in future studies.

Overall, the results confirm the potential of analytical modeling approaches for fast prediction of cantilever distortions and the importance of scanning strategy selection for laser cladding on thin-walled base material. Improved manufacturing strategies and sequences can lead to increased shape accuracies, from which many industrial applications can benefit.

4 Conclusions

This study describes an analytical approach to model longitudinal substrate bending and experimentally evaluates the effect of clad height, substrate thickness and deposition strategies on cantilever distortion. The modeling results show that the analytical model can efficiently predict longitudinal bending after calibration with experimental data. The experimental results lead to the following conclusions:

- Increased clad heights lead to increased distortion. The contribution of the lowest deposited layers is largest. Therefore, for distortion-critical substrates, the lowest

layers should be deposited with processing parameters that lead to a minimum amount of residual stress.
- Increased substrate thickness results in a reduction of both longitudinal bending and angular distortion.
- For thin-walled substrates, there is a large effect of the scanning strategy on the final cantilever distortion, as angular distortion contributes to a larger amount of deflections. Manufacturing strategies with longitudinal scanning in the present study reduced distortions by up to 86 %. Therefore, longitudinal scanning directions should be considered for laser cladding on thin substrates.
- Future work will focus on the validation of FEA-based thermo-mechanical models with an optimized experimental setup and on the application of distortion mitigation strategies for complex part manufacturing by DMD.

Declarations

References

1. Rettberg R, Kraenzler T (2021) Hybrid manufacturing: a new additive manufacturing approach for closed pump impellers. In: Industrializing Additive Manufacturing, pp 146–159. https://doi.org/10.1007/978-3-030-54334-1_11

2. DebRoy T, Mukherjee T, Milewski JO, Elmer JW, Ribic B, Blecher JJ, Zhang W (2019) Scientific, technological and economic issues in metal printing and their solutions. Nat Mater 18(10):1026–1032. https://doi.org/10.1038/s41563-019-0408-2

3. DebRoy T, Wei HL, Zuback JS, Mukherjee T, Elmer JW, Milewski JO, Beese AM, Wilson-Heid A, De A, Zhang W (2018) Additive manufacturing of metallic components – Process, structure and properties. Prog Mater Sci 92:112–224. https://doi.org/10.1016/j.pmatsci.2017.10.001

4. Eisenbarth D, Borges Esteves PM, Wirth F, Wegener K (2019) Spatial powder flow measurement and efficiency prediction for laser direct metal deposition. Surf Coat Technol 362:397–408. https://doi.org/10.1016/j.surfcoat.2019.02.009

5. Woo W, Kim D-K, Kingston EJ, Luzin V, Salvemini F, Hill MR (2019) Effect of interlayers and scanning strategies on through-thickness residual stress distributions in additive manufactured ferritic-austenitic steel structure. Mat Sci Eng A 744:618–629. https://doi.org/10.1016/j.msea.2018.12.078

6. Gray T, Camilleri D, McPherson N (2014) Understanding welding distortion: thermal fields thermo-mechanical effects. In: Control of Welding Distortion in Thin-Plate Fabrication, pp 53–76. https://doi.org/10.1533/9780857099327.53

7. Ng GKL, Jarfors AEW, Bi G, Zheng HY (2009) Porosity formation and gas bubble retention in laser metal deposition. Applied Physics A 97(3):641–649. https://doi.org/10.1007/s00339-009-5266-3

8. Wirth F (2019) Process understanding, modeling and predictive simulation of laser cladding. Dissertation, ETH Zürich

9. Soffel F, Eisenbarth D, Hosseini E, Wegener K (2021) Interface strength and mechanical properties of Inconel 718 processed sequentially by casting, milling, and direct metal deposition. J Mater Process Technol 291:117021. https://doi.org/10.1016/j.jmatprotec.2020.117021

10. Eisenbarth D, Soffel F, Wegener K (2019) Effects of direct metal deposition combined with intermediate and final milling on part distortion. Virtual Phys Prototyp 14(2):130–134. https://doi.org/10.1080/17452759.2018.1532799

11. Mukherjee T, Zuback JS, De A, DebRoy T (2016) Printability of alloys for additive manufacturing. Sci Rep 6:19717. https://doi.org/10.1038/srep19717

12. Heigel JC, Michaleris P, Palmer TA (2015) In situ monitoring and characterization of distortion during laser cladding of Inconel® 625. J Mater Process Technol 220:135–145. https://doi.org/10.1016/j.jmatprotec.2014.12.029

13. Ren K, Chew Y, Fuh JYH, Zhang YF, Bi GJ (2019) Thermo-mechanical analyses for optimized path planning in laser aided additive manufacturing processes. Mater Des 162:80–93. https://doi.org/10.1016/j.matdes.2018.11.014

14. Lu X, Lin X, Chiumenti M, Cervera M, Hu Y, Ji X, Ma L, Yang H, Huang W (2019) Residual stress and distortion of rectangular and s-shaped Ti-6Al-4V parts by directed energy deposition: modelling and experimental calibration. Addit Manuf 26:166–179. https://doi.org/10.1016/j.addma.2019.02.001

15. Xie R, Chen G, Zhao Y, Zhang S, Yan W, Lin X, Shi Q (2019) In-situ observation and numerical simulation on the transient strain and distortion prediction during additive manufacturing. J Manuf Process 38:494–501. https://doi.org/10.1016/j.jmapro.2019.01.049

16. Yan Z, Liu W, Tang Z, Liu X, Zhang N, Wang Z, Zhang H (2019) Effect of thermal characteristics on distortion in laser cladding of AISI 316L. J Manuf Process 44:309–318. https://doi.org/10.1016/j.jmapro.2019.06.011

17. Denlinger ER, Michaleris P (2016) Effect of stress relaxation on distortion in additive manufacturing process modeling. Addit Manuf 12:51–59. https://doi.org/10.1016/j.addma.2016.06.011

18. Yang Q, Zhang P, Cheng L, Min Z, Chyu M, To AC (2016) Finite element modeling and validation of thermomechanical behavior of Ti-6Al-4V in directed energy deposition additive manufacturing. Addit Manuf 12:169–177. https://doi.org/10.1016/j.addma.2016.06.012

19. Xie R, Zhao Y, Chen G, Zhang S, Lin X, Shi Q (2019) Development of efficient distortion prediction numerical method for laser additive manufactured parts. J Laser Appl 31(2):022314. https://doi.org/10.2351/1.5096147

20. Biegler M, Elsner BAM, Graf B, Rethmeier M (2020) Geometric distortion-compensation via transient numerical simulation for directed energy deposition additive manufacturing. Sci Technol Weld Join 25(6):468–475. https://doi.org/10.1080/13621718.2020.1743927

21. Shen H, Yao Z, Shi Y, Hu J (2006) An analytical formula for estimating the bending angle by laser forming. Proc Inst Mech Eng C - J Mech E 220:243–247. https://doi.org/10.1243/095440606X79721

22. Mercelis P, Kruth JP (2006) Residual stresses in selective laser sintering and selective laser melting. Rapid Prototyp J 12(5):254–265. https://doi.org/10.1108/13552540610707013

23. Mukherjee T, Manvatkar V, De A, DebRoy T (2017) Mitigation of thermal distortion during additive manufacturing. Scr Mater 127:79–83. https://doi.org/10.1016/j.scriptamat.2016.09.001

24. Xie D, Zhao J, Liang H, Tian Z, Shen L, Xiao M, Ahsan MN, Wang C (2018) Assumption of constraining force to explain distortion in laser additive manufacturing. Materials 11(11):2327. https://doi.org/10.3390/ma11112327

25. Liang X, Cheng L, Chen Q, Yang Q, To AC (2018) A modified method for estimating inherent strains from detailed process simulation for fast residual distortion prediction of single-walled structures fabricated by directed energy deposition. Addit Manuf 23:471–486. https://doi.org/10.1016/j.addma.2018.08.029